Optics Communications 525 (2022) 128802

Contents lists available at ScienceDirect

Optics Communications

journal homepage: www.elsevier.com/locate/optcom

Employing spin noise spectroscopy of rubidium ensemble to calibrate Hall magnetometers when measuring weak magnetic fields

Yongbiao Yang [a], Lulu Zhang [a], Lele Bai [a], Jun He [a,b,c], Yanhua Wang [a,c], Junmin Wang [a,b,c,*]

[a] State Key Laboratory of Quantum Optics and Quantum Optics Devices, and Institute of Opto-Electronics, Shanxi University, Tai Yuan 030006, China
[b] Collaborative Innovation Center of Extreme Optics, Shanxi University, Tai Yuan 030006, China
[c] School of Physics and Electronic Engineering, Shanxi University, Tai Yuan 030006, China

ARTICLE INFO

Keywords:
Spin noise spectroscopy
Hall magnetometer
Calibration
Rubidium atoms
Signal-to-noise ratio

ABSTRACT

Accuracy, deviation, and zero points drifting of commercial Hall magnetometers are important limiting factors and need to be calibrated, especially for measuring weak magnetic fields at micro Tesla level. Here, we present that measurement and characterization of spin noise spectroscopy (SNS) with a rubidium atomic ensemble under good magnetic shielding condition and its application for calibration of commercial Hall magnetometers. Obtaining SNS with narrow linewidth and high signal-to-noise ratio (SNR) is crucial to improve the accuracy of calibration. In experiment, we measured SNS with a rubidium vapor cell coated with paraffin on the inner wall, analyzed SNS signals and linewidth with different probe intensity and probe frequency detuning, and optimized these parameters for reducing the errors. Under different transverse magnetic fields generated by magnetic coils driven by an ultra-low noise and high-precision constant current source, SNS signals of rubidium atomic ensemble are measured. Corresponding Larmor frequency can be derived by fitting SNS signal, therefore transverse magnetic fields can be calibrated. We compared the transverse magnetic fields calibrated by SNS with those measured by the Hall magnetometer, analyzed the deviation and accuracy, and obtained calibration factor of commercial Hall magnetometer we used. This method is very simple and easily implemented, and can also be extended to calibrate commercial fluxgate magnetometers.

1. Introduction

Magnetic fields measurement is increasingly significant in geological exploration, space exploration, searching dark matter, and etc [1]. Therefore, a large number of related studies on high-sensitivity magnetometers have been carried out successively [1,2]. And various types of commercial magnetometers are developed for actual requirement of magnetic fields measurement in laboratories, such as Hall magnetometer, fluxgate magnetometer, optically pumped cesium magnetometer, and etc. Commercial Hall magnetometers can satisfy magnetic fields measurement from micro Tesla to dozens of Tesla. However, commercial Hall magnetometers always exist zero points drifting, and also exist problems of large deviation and poor accuracy, especially for measuring weak magnetic fields at micro Tesla level, resulting in larger errors in measuring weak magnetic fields. And a traditional method is usually to place the magnetic probe in a magnetic shielding barrel and reset it to zero for calibration, it can reduce zero points drifting, but is powerless for deviation and accuracy.

Spin noise spectroscopy (SNS) [3] is a technique that reflects atomic fluctuations based on the rotation of the polarization plane of linearly polarized light with frequency detuning in an ensemble of thermal equilibrium. As early as 1946, Bloch proposed that atoms had spin fluctuations [4]. In 2004, Crooker et al. demonstrated measurement of SNS of rubidium and potassium atomic vapor based on Faraday rotation effect [5]. As a kind of perturbation-free magnetic resonance techniques, SNS not only can well reveal some physical properties of atoms [6], such as spin coherence lifetime, hyperfine splitting and Lande factor, but also be used to measure some specific magnetic fields. Thus have been widely studied and applied [7–9], especially in the fields of semiconductor research [10]. Spin fluctuations precess with Larmor frequency under a given external transverse magnetic field, and peak value of SNS corresponds to Larmor frequency, it is important for SNS with narrow linewidth and high signal-to-noise ratio(SNR) to use Lorentz function to derive the precise Larmor frequency. The linewidth of SNS represents the spin transverse relaxation time of the atoms. Violent collision between atoms with thermal motion and the inner wall of the vapor cell will greatly destroy the state of random polarization of spin fluctuations. Coating the inner wall with anti-spin relaxation film such as paraffin and OTS film [11] or filling with high-pressure

* Corresponding author at: State Key Laboratory of Quantum Optics and Quantum Optics Devices, and Institute of Opto-Electronics, Shanxi University, Tai Yuan 030006, China.
E-mail address: wwjjmm@sxu.edu.cn (J. Wang).

https://doi.org/10.1016/j.optcom.2022.128802
Received 8 June 2022; Received in revised form 13 July 2022; Accepted 18 July 2022
Available online 26 July 2022

buffer gas [12] and fluorescent quenching gas such as nitrogen both can effectively protect spin state of the atoms during the diffusion process, greatly increases spin transverse relaxation time of the atoms, and obtains SNS with relatively narrow linewidth; Additionally, polarized squeezed light can break through the shot noise limit of probe light [13,14] and improve SNR of atomic SNS.

In this paper, we use cubic atomic vapor cell filled with natural abundance rubidium atoms and coated with paraffin on the inner wall in experiment. Signals and full width at half maximum of SNS under different intensity and frequency detuning of probe beam were compared, optimized these parameters for reducing the errors. Corresponding Larmor frequency can be derived by fitting SNS signal, and magnetic fields given by SNS were used to evaluate and calibrate the commercial Hall magnetometers. The success of this work depends on a good magnetic shielding environment and particularly stable magnetic fields.

2. Experimental principle and apparatus

2.1. Experimental principle

If "N_+" is used to represent the number of spin-up particles, and "N_-" is used to represent the number of spin-down particles, the atomic spin polarization can be described N_+-N_-/N_++N_-. In the thermal equilibrium atomic ensemble, macroscopic spin polarization manifests as zero, but random fluctuations inherent to the spins induce macroscopic magnetic moment to fluctuate and appears as spontaneous spin polarization, the polarization vector precesses at Larmor frequency around the external magnetic field. A linearly polarized light passing through atomic vapor cell can be regarded as a combination of left-circularly polarized component and right-circularly polarized component. The index of refraction for two components is different in the medium since effect of spontaneous spin polarization, which causes left-circularly component and right-circularly component to have different phases when them leave atomic vapor cell, as a result, the polarization plane of the outgoing linearly polarized light is rotated. The spin precession of spontaneous spin polarization in the magnetic field is detected by Faraday rotation of the linearly polarized light. And frequency of the precession signal and external magnetic field satisfies the relationship $\nu_L=\mu_B$gB/h [5], where h is Planck's constant, g is the Lande factor of the ground state of the ^{85}Rb, μ_B is the Bohr magneton, and B is the magnitude of external transverse magnetic field. By fitting the Lorentz function to accurately derive the peak frequency, the value of the magnetic field can be determined.

2.2. Experimental apparatus

A 795-nm grating external-cavity diode laser (ECDL) was used in our experiment, the output laser beam was coupled through a single-mode fiber, and then via a Glan prism with high extinction ratio to obtain linearly polarized light. The linearly polarized light passed through a rubidium vapor cell, and then passed through a polarimeter consist of a $\lambda/2$ wave plate and a Wollaston prism, was received by a balanced differential detector. The Wollastom prism split the linearly polarized light into two beams with s and p polarization. Before applying a transverse magnetic field, adjust $\lambda/2$ wave plate to keep two beams have the same intensity, after the transverse magnetic fields were applied, the two beams entered the detector and exported a differential signal, which carried the information of Faraday rotation angle of polarization plane. The output signals were collected and then SNS of rubidium atoms were recorded and analyzed by a Fast-Fourier-Transformation (FFT) dynamic signal analyzer.

During the experiment, the rubidium vapor cell was placed inside a 4 μ-metal layers of magnetic shield apparatus, effectively reduced the disturbance caused by geomagnetic field and other ambient magnetic fields. A precision current source (Keysight B2961A) with lower noises provided currents to a Helmholtz coil to generate stable and uniform magnetic fields transverse to the laser direction. Using alternating current through a non-magnetic electric heater to heat rubidium vapor cell and control the temperature. In order to obtain SNS with higher SNR, experimental data were averaged multiple times, and then collected and processed through the FFT dynamic signal analyzer.

We used cubic atomic vapor cell with a size of 20 mm × 20 mm × 20 mm filled with natural abundance rubidium atoms(Rb 85: 72.15%; Rb 87: 27.85%). The inner walls of the vapor cell were coated with paraffin as an anti-spin relaxation film. The temperature of the vapor cell was controlled at 44 °C to create a atomic number density of $8.4 \times 10^{10}/cm^3$. Since the number density of ^{87}Rb atoms in the cell are much smaller than that of ^{85}Rb atoms, in order to obtain the SNS with better SNR, only SNS of ^{85}Rb atoms is used to the calibrate Hall magnetometer in the experiment. Experimental data and errors were collected separately for the external magnetic fields applying and turning off, the difference between them as final measurement results to eliminate some other inherent noises(such as detector noise) and improve SNR of SNS.

As shown in Fig. 1(b), the power of the incident linearly polarized light was 1 mW, and the probe beam was blue detuned by 600 MHz from the ^{85}Rb $5S_{1/2}$(F=3)-$5P_{1/2}$(F'=2) transition, with the external transverse magnetic field of 9.45 μT, SNS of the ^{85}Rb atoms was obtained, the black line was measured data, the red curve was the result of fitting with the Lorentz function, and Larmor frequency corresponding to the peak was 44.34 kHz, and resonant width at half maximum of SNS was 5.08 kHz. Using the formula $\nu_L=\mu_B$gB/h [5], the value of external transverse magnetic field can be verified. And the narrower linewidth of SNS, the more accurate for the fitting of Larmor frequency, and errors caused by the calibrating Hall magnetometers are smaller.

3. Experiment result

3.1. Noise signals and linewidth of spin noise spectrum with different probe optical powers

SNS of rubidium atoms is not limited by the ambient and human factors for the calibration of the magnetic fields, and its characteristics that reveal magnetic fields come from the properties of atoms themselves, so there is no deviation in the calibration magnetic field by SNS. However, limited that SNR and linewidth of SNS is not ideal, fitting Larmor frequency corresponding to the peak has errors. The fitting result depends not only on the signal of spin noise and background noise, but also on the linewidth of SNS. It can be imagined that SNS with high SNR and narrow linewidth is crucial for accurately fitting Larmor frequency. By increasing the probe power and changing the frequency detuning to improve SNR of SNS and change its linewidth and make fitting results of Larmor frequency more accurate.

The probe beam was blue detuned by 600 MHz from the $5S_{1/2}$(F=3)-$5P_{1/2}$(F'=2) transition of the ^{85}Rb atoms, and SNS of the ^{85}Rb atoms obtained under different powers of probe beam were compared. Keeping other conditions being the same, with the increase of powers of the probe beam from 0.4 mW to 2 mW, the signals of SNS were increasing. SNS was integrated to obtain the spin fluctuation signals of the ^{85}Rb, and background noises were also integrated, we analyzed the relationship between spin noise of atoms and the light intensity of the probe, and the relationship between background noise and light intensity. It can be found by fitting (Fig. 2(c) and Fig. 2(d)), spin noises have a linear relationship with the square of the probe-beam intensity, while background noises have a linear relationship with the probe-beam intensity. This is mainly because signals detected by balanced differential detector have a linear relationship with the light intensity, when performing FFT, the mode square of time domain signals are taken to obtain the power spectral density, resulting in a linear relationship between the spin noise power spectrum and the square of probe-beam intensity [15]. The background noise is used as

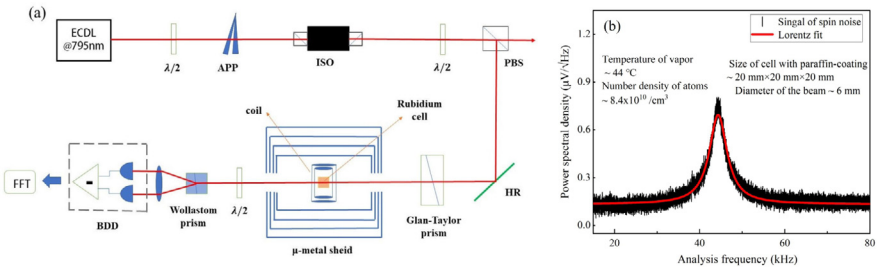

Fig. 1. (a) Schematic diagram of experimental setup. APP: anamorphic prisms pair; PBS: polarization beam splitter cube; $\lambda/2$: half-wave plate; ISO: isolator; HR: high-reflectivity mirror; BDD: balanced differential detector; FFT:Fast-Fourier-Transformation; (b) Typical spin noise spectrum of ^{85}Rb atomic ensemble.

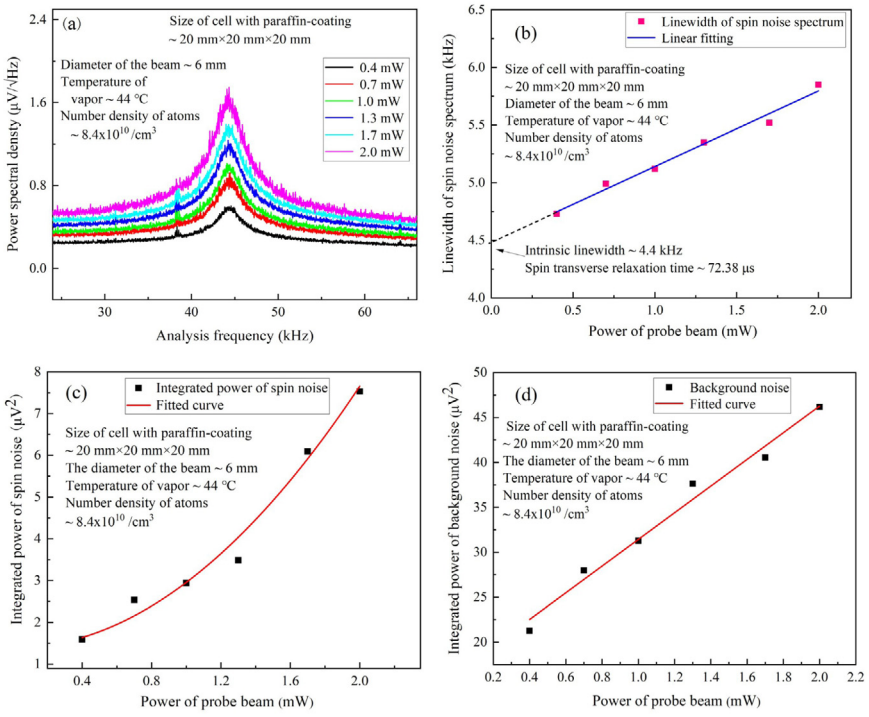

Fig. 2. (a) SNS of ^{85}Rb atomic ensemble relative to different probe beam's powers (diameter of the probe beam 6 mm, and the temperature of the rubidium vapor was controlled at 44 °C, the probe beam was blue detuned by 600 MHz from ^{85}Rb $5S_{1/2}$ (F=3) -$5P_{1/2}$ (F'=2) transition, and external transverse magnetic field is 9.4 μT). (b) The dependence of the linewidth of SNS on the powers of probe beam, the intercept of linear fitting is 4.4 kHz, corresponding to a spin transverse relaxation time of 72.38 μs,.

the noise limit for measuring the rotation angle of the polarization plane of the probe beam, mainly the shot noise of photons. If the shot noise of photons is described by Δn, then shot noise of photons can be written as $\Delta n \sim \sqrt{N}$ [16], where $N=p/h\nu$ is average photons number, and p is the power of the probe beam, so the shot noise of photons dominating background noise is proportional to square root of the probe-beam intensity [17,18]. After FFT, the integrated background noise is proportional to the probe-beam intensity.

For SNR of the rubidium SNS, it can be defined by the ratio of the spin noise amplitude to the standard deviation of the background noise [17]. As the powers of probe beam increase, the SNR of SNS will increase, so as to obtain more accurate transverse magnetic fields, in addition, the linewidth of SNS will also broaden. As shown in Fig. 2(b), the broadening is proportional to the power of probe beam. It is because that ground state atoms absorb near-resonant photons, so that the spin precession of the ground state rubidium atoms is interrupted, that is, the optical pumping effect. Linearly extrapolated to the power of probe beam is zero, the intrinsic linewidth of 4.40 kHz is obtained, from this, the actual spin transverse relaxation time of rubidium atoms is 72.38 μs, and the power broadening is 650 Hz/mW, which also has a negative effect on the accurate fitting of the peak frequency. Therefore, while pursuing a high SNR, it is necessary to take into account the linewidth broadening of SNS.

3.2. Noise signals and linewidth of spin noise spectrum with different frequency detuning

The frequency detuning of probe beam relative to the center frequency of transition of the rubidium atoms is different can cause varying degrees of perturbation of the linearly polarized light to the atomic ensemble, so the magnitude of spin fluctuations and the frequency detuning amount will have certain dependence. Stabilizing the temperature of the rubidium vapor cell, the power and diameter of the probe beam remained unchanged, zero detuning means ^{85}Rb $5S_{1/2}$(F=3)-$5P_{1/2}$(F'=2) transition was used as the center frequency, and the frequency of the probe beam was changed in near-resonance transition range of a few hundred MHz. After the probe beam with different frequency detuning passed through the rubidium vapor cell, the signals of spin fluctuations carried by the polarization plane of the linearly polarized light were compared, signals were averaged 2000 times for each measurement. As shown in Fig. 3(a), the experimental results showed that spin noise of atoms are changing with different frequency detuning, and signals of spin noise have a maximum value relative frequency detuning.

Since the absorption of light by atoms is very weak, the probe beam mainly senses the fluctuation of ground state atoms through refraction.

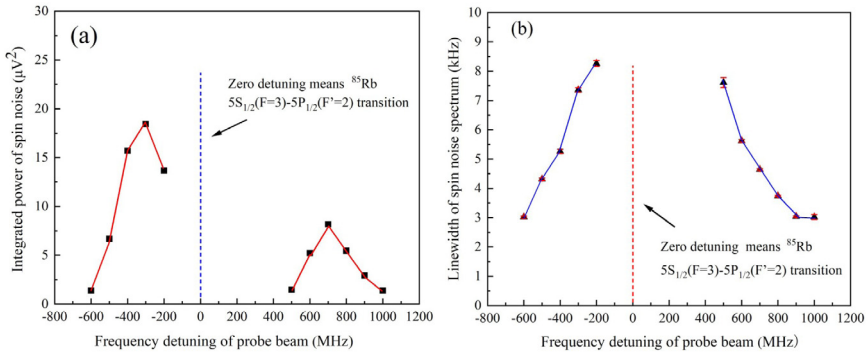

Fig. 3. (a) The integrated spin noise versus the probe beam's frequency detuning. (b) Linewidth of SNS versus the probe beam's frequency detuning. (Power of the probe beam 1 mW, diameter of the probe beam 6 mm, and the temperature of the rubidium vapor is controlled at 44 °C, and zero detuning means the probe beam is resonant to the ^{85}Rb $5S_{1/2}$ (F = 3) - $5P_{1/2}$ (F'=2) transition.)

As the frequency detuning of the probe beam changes, the absorption of the probe light by the atoms is also different, result in the number of particles in the Zeeman sub-energy level of the ground-state atom to redistribute, so that the index of refraction of left and right circularly polarized light is different [3], and there exist extreme values, so the spin fluctuation signals of the atoms are also different. In addition, the signals of SNS are asymmetric to the detuned features, which is caused by the coupling of atomic energy levels under near-resonant probe conditions.

It can be seen from this that choosing appropriate frequency detuning can improve SNR of SNS. At the same time, with the increase of the frequency detuning amount, as shown in Fig. 3(b), the linewidth of SNS will become narrower, the main reason is also that increasing the frequency detuning of the probe beam reduces the disturbance of the atomic ensemble caused by the optical pumping effect, and increases the spin transverse relaxation time of the atoms. Increasing the frequency detuning amount of the probe beam ensures that the linewidth of SNS is narrower while taking into account a higher SNR, which is also an effective method for accurately fitting the SNS of the ^{85}Rb atoms and deriving the Larmor precession frequency to obtain accurate magnetic fields.

3.3. Measurement errors and calibration of different magnetic fields

The Hall magnetometer used in our experiment is a single-axis magnetometer manufactured by Lake Shore(Model 455DSP) and has two magnetic induction probes which measure magnetic fields in different direction, the measurement range of the magnetic fields is 3.5 μT–35 T. In the experiment, we used the Hall magnetometer to measure the transverse magnetic fields, before measuring magnetic fields every time, the magnetometer needs to reset zero, which put the magnetic probe inside the magnetic shield device to reset zero. This magnetic shied device provides a good zero-field condition with residual magnetism about a few Nano Tesla, meanwhile, benefit by a very stable static magnetic field, provided by an ultra-low noise and high-precision constant current source, ensuring the reliability of the experiment. Probe of the Hall magnetometer was placed in the original position of the atomic cell, then employing SNS of rubidium ensemble to evaluated and calibrated measurement results of the Hall magnetometer.

The same currents were applied to the magnetic field coil, and measurement results of the Hall magnetometer were compared with the transverse magnetic field obtained by using SNS of the ^{85}Rb atoms. We provided the measurement results and measurement errors with different currents and compared results and relative errors of the magnetic fields measurement in Table 1, it showed that the measurement results of the commercial Hall magnetometer were slightly larger than the magnetic field values of the real environment, and the measurement errors are also larger, indicating that the accuracy of the Hall magnetometer is not very high and its measuring deviation is large in measuring weak magnetic fields, which brings unfavorable factors to the judgment of the magnetic fields conditions during experiments. Thus highlighting the necessity that calibrating the Hall magnetometer. We demonstrated measurement errors of magnetic fields by using SNS far below that the measurement of Hall magnetometer (in Fig. 4(a) and (b)) and it is available that employing SNS to calibrate Hall magnetometers. We also analyzed the relative deviation of magnetic fields measured by the Hall magnetometer relative to the calibration of SNS. Fig. 4(d) showed that the relative deviation of the Hall magnetometer varies with different currents.

Table 1
The transverse magnetic field values calibrated by rubidium-85 atoms' SNS and transverse magnetic field values measured by the Hall magnetometer with different currents applied to the magnetic coils.

Current values in the magnetic coils (mA)	60	230	350	600	700	900	1150	1300
Magnetic field values given by the Hall magnetometer (μT)	7.686 ±0.197	29.271 ±0.140	44.346 ±0.162	76.345 ±0.210	88.934 ±0.329	114.427 ±0.208	146.250 ±0.138	165.142 ±0.145
Larmor frequency value of ^{85}Rb atoms given by fitting SNS (kHz)	35.384 ±0.032	136.397 ±0.025	207.271 ±0.019	353.825 ±0.055	414.419 ±0.048	534.141 ±0.031	681.771 ±0.027	770.868 ±0.029
SNS' linewidth (kHz)	4.579 ±0.107	3.907 ±0.074	5.086 ±0.057	6.310 ±0.158	6.667 ±0.139	5.668 ±0.090	6.101 ±0.078	6.209 ±0.086
Magnetic field values given by SNS (μT)	7.545 ±0.007	29.082 ±0.006	44.194 ±0.004	75.282 ±0.012	88.362 ±0.010	113.889 ±0.007	145.367 ±0.006	164.364 ±0.006

We optimized experimental parameters to improve SNR of SNS and reduce its linewidth, making measuring errors greatly reduced. The magnetic fields generated by Helmholtz coil have a linear relationship with the currents providing the magnetic fields. We measured transverse magnetic fields in optimal parameters conditions with different currents by employing SNS of rubidium ensemble, and then measured the magnetic fields provided that same currents by using the Hall magnetometer. We have both performed a linear fit, fitting the results measured by the Hall magnetometer to obtain the scale factor k_1=0.12709 of the magnetic field and current; fitting the results employing SNS to obtain the scale factor k_2=0.12642, thus we defined calibration factor C to calibrate the measurement results of the Hall magnetometer, where $C=k_2/k_1$, then calibrated magnetic field value can be $B'=B_0*C$, where B_0 is values measured by the Hall magnetometer, achieved the calibration of commercial Hall magnetometers measurements employing SNS of rubidium ensemble.

The linewidth of SNS will change with transverse magnetic field of varying strength are applied, which is mainly caused by inhomogeneity of magnetic fields at the location of the rubidium vapor cell [19]. The Larmor frequency of atoms in different parts of the cell is different, which increases the linewidth of the SNS by reducing the transverse

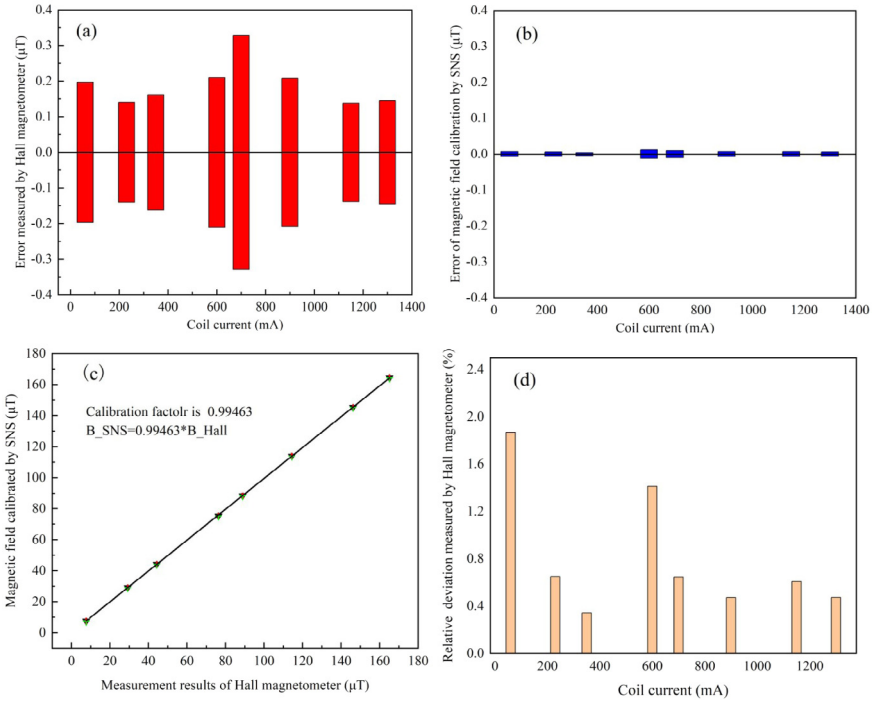

Fig. 4. (a) Measuring errors of magnetic fields of different coil currents by using Hall magnetometer. (b) Measuring errors of calibrating magnetic fields of different coil currents by SNS. (c) The relationship between the magnetic fields calibrated by SNS and the measurement results of the Hall magnetometer. (d) The relative deviation of the measurement result of Hall magnetometer from the calibration result of SNS.

relaxation time. The inhomogeneity of magnetic fields felt by atoms also showed in the cell filled with high pressure buffer gas, which likely to cause moving of Larmor frequency. In addition, polarization squeezed light at 795 nm as the probe beam was compared with probe of coherent light field under the same experimental conditions. The squeezed light was prepared based on optical parametric oscillation (OPO) [14]. Using polarization squeezed light as probe can enhance SNR of SNS beyond the photon shot noise level without changing its linewidth [14,15]. Comparing with probe of coherent light field, squeezed light as probe is more accurate for fitting the Larmor frequency, and the calibration results of the Hall magnetometer have smaller errors and higher accuracy. Considering that the frequency accuracy of the FFT spectrometer may bring some errors in determining the absolute frequency of SNS, we may be able to use a rubidium atomic clock(SRS FS-725) to calibrate the FFT spectrometer, where the frequency stability of the rubidium atomic clock is better than 1E-11, so that the influence of the instrument on the absolute frequency of SNS is much less than the effect of SNR and linewidth.

4. Conclusion

We demonstrated employing SNS of rubidium ensemble to calibrate the Hall magnetometers when measuring weak fields, which has been accomplished in a good magnetic shielding environment. Typical linewidth of SNS of the ^{85}Rb atoms is about 5.1 kHz. SNR of SNS can be appropriately improved by changing the power and detuning frequency of the probe beam. SNS with narrow linewidth and high SNR is suitable for fitting accurate Larmor frequency and obtaining precise magnetic field values. After measuring the transverse magnetic fields using the Hall magnetometer and comparing the transverse magnetic field values derived by SNS with those measured by the Hall magnetometer, we analyzed the measurement deviation of the Hall magnetometer, therefore employed SNS of rubidium atoms to calibrate the Hall magnetometer when measuring weak magnetic fields. Using SNS of atoms to calibrate the commercial Hall magnetometers has the advantages of simple device and convenient operation. This method can also be extended to calibrate the fluxgate magnetometers.

Declaration of competing interest

The authors declare that they have no known competing financial interests or personal relationships that could have appeared to influence the work reported in this paper.

Data availability

Data will be made available on request.

Acknowledgments

This work was financially supported by the National Key R&D Program of China (Grant No. 2017YFA0304502) and the National Natural Science Foundation of China (Grant Nos. 11974226 and 61875111).

References

[1] D. Budker, D.F.J. Kimball, Optical Magnetometry, Cambridge University Press, 2013.
[2] W.M. Sun, S.Q. Liu, W.H. Zhao, J.H. Zhang, Guang Xue Yuan Zi Ci Li Yi (Optical Atomic Magnetometers), Harbin Engineering University Press, 2014, in Chinese.
[3] V.S. Zapasskii, Spin-noise spectroscopy: From proof of principle to applications, Adv. Opt. Photonics 5 (2013) 131–168.
[4] F. Bloch, Nuclear induction, Phys. Rev. 70 (1946) 460–474.
[5] S.A. Crooker, D.G. Rickel, A.V. Balatsky, D.L. Smith, Spectroscopy of spontaneous spin noise as a probe of spin dynamics and magnetic resonance, Nature 431 (2004) 49–52.
[6] Y.L. Yang, L.L. Bai, L.L. Zhang, J. He, X. Wen, J.M. Wang, Experimental investigation of spin noise spectroscopy of rubidium atomic ensemble, Acta Phys. Sin. 69 (2020) 233201, in Chinese.
[7] H. Horn, G.M. Müller, E.M. Rasel, L. Santos, J. Hübner, M. Oestreich, Spin-noise spectroscopy under resonant optical probing conditions: Coherent and nonlinear effects, Phys. Rev. A 84 (2011) 043851.
[8] Z.C. Guo, T.Y. Zhang, J. Zhang, Spin noise spectroscopy of cesium vapor in micron-scale cell, Acta Phys. Sin. 69 (2020) 037201, in Chinese.
[9] S.M. Song, M. Jiang, Y.S. Qin, Y. Tong, W.Z. Zhang, X. Qin, R.B. Liu, X.H. Peng, Collision-sensitive spin noise, Phys. Rev. Appl. 17 (2022) L011001.
[10] M. Römer, J. Hübner, M. Oestreich, Spin noise spectroscopy in semiconductors, Rev. Sci. Instrum. 78 (2007) 103903.

[11] Y. Tang, Y. Wen, L. Cai, K.F. Zhao, Spin-noise spectrum of hot vapor atoms in an anti-relaxation-coated cell, Phys. Rev. A 101 (2020) 013821.
[12] V.G. Lucivero, N.D. McDonough, N. Dural, M.V. Romalis, Correlation function of spin noise due to atomic diffusion, Phys. Rev. A 96 (2017) 062702.
[13] V.G. Lucivero, R.J. Martínez, J. Kong, M.W. Mitchell, Squeezed-light spin noise spectroscopy, Phys. Rev. A 93 (2016) 053802.
[14] L.L. Bai, L.L. Zhang, Y.B. Yang, R. Chang, Y. Qin, J. He, X. Wen, J.M. Wang, Enhancement of spin noise spectroscopy of rubidium atomic ensemble by using the polarization squeezed light, Opt. Express 30 (2022) 1925–1935.
[15] Y.X. Shang, J. Ma, P. Shi, X. Qian, W. Li, Y. Ji, Measurement and improvement of rubidium spin noise spectroscopy, Acta Phys. Sin. 67 (2018) 087201, in Chinese.
[16] G.E. Katsoprinakis, A.T. Dellis, I.K. Kominis, Measurement of transverse spin-relaxation rates in a rubidium vapor by use of spin-noise spectroscopy, Phys. Rev. A 75 (2007) 042502.
[17] H.Y. Yang, Research on the Basic Physical Process Based on Hot Atom Spin and the Application of Magnetometer, (Ph.D. thesis), Graduate School of Chinese Academy of Engineering Physics, 2020, in Chinese.
[18] P. Shi, J. Ma, X. Qian, Y. Ji, W. Li, Signal-to-noise ratio of spin noise spectroscopy in rubidium vapor, Acta Phys. Sin. 66 (2017) 017201, in Chinese.
[19] P.X. Miao, S.Y. Yang, J.X. Wang, J.Q. Lian, J.H. Tu, W. Yang, J.Z. Cui, Rubidium atomic magnetometer based on pump-probe nonlinear magneto-optical rotation, Acta Phys. Sin. 65 (2016) 210702, in Chinese.